Modeling and Analysis

GREENHOUSE GASES SCIENCE AND TECHNOLOGY

Statistical performance of CO_2 leakage detection using seismic travel time measurements

Zan Wang and Mitchell J. Small, Carnegie Mellon University, Pittsburgh, PA, USA

Abstract: Monitoring for possible CO_2 leakage is an important part of a safe and effective geological sequestration program. Seismic monitoring has been implemented in several pilot sequestration sites for site characterization and CO_2 leakage detection. This study evaluates the detection power of seismic wave travel time measurements and statistical tests at different CO_2 leakage rate levels. A simplified rock physics model is assumed for monitoring zones at sequestration sites and the effects of leakage-induced changes in pressure and CO_2 saturation on P-wave travel times are modeled. The empirical distributions of detection power using the P-wave travel time for four regions in the permeability-porosity input space at four leakage levels are obtained from the Monte Carlo uncertainty analysis with a stochastic response surface method. The detection power using the P-wave travel time measurements and test alone is generally not high enough, unless the porosity and the permeability of the monitoring zone are high, and/or a long period of time has elapsed since the leakage occurred. For monitoring layers with lower permeability and porosity, measurements from other monitoring techniques will likely be needed to increase the probability that leakage events are detected and addressed in a timely manner. © 2015 Society of Chemical Industry and John Wiley & Sons, Ltd

Keywords: carbon sequestration; leakage detection; seismic monitoring; seismic travel time; statistical power

Introduction

It is estimated that the atmospheric carbon has increased by 240 ± 10 PgC between 1750 and 2011.[1] Most of the increase is due to emissions from fossil fuel combustion and cement production.[1] Geological carbon sequestration in which CO_2 is injected and remains permanently stored in a subsurface formation is considered a promising initial option to slow or reduce global atmospheric CO_2 concentrations.[2]

Monitoring for possible CO_2 leakage is an important part of a safe and effective geological sequestration program.[3] An overview of available monitoring techniques is provided in the report of the US Department of Energy on Monitoring, Verification, and Accounting of CO_2 Stored in Deep Geologic Formations.[3] Monitoring techniques can be categorized into atmospheric monitoring methods, near-surface monitoring methods, and deep-subsurface monitoring methods based on the depth where these techniques are deployed.[3,4] The performance of near-surface monitoring techniques, including soil CO_2 flux measurements and tracer measurements, has been evaluated by Yang *et al.* using a Bayesian belief

Correspondence to: Zan Wang, Department of Civil & Environmental Engineering, Carnegie Mellon University, 5000 Forbes Avenue, Pittsburgh, PA 15213, USA. E-mail: zanw@andrew.cmu.edu
Received February 25, 2015; revised July 1, 2015; accepted August 6, 2015
Published online at Wiley Online Library (wileyonlinelibrary.com). DOI: 10.1002/ghg.1533

network approach.[5–7] Pressure monitoring, a widely used subsurface monitoring technique, has also been extensively studied.[8–13] A methodology for detecting CO_2 leakage through abandoned wells was developed using pressure and surface-deformation measurements.[14] It is generally found that the individual monitoring techniques studied are unlikely to provide sufficient statistical power for CO_2 leakage detection, so that multiple monitoring techniques may need to be utilized together at a site.[5,6,8,9]

Seismic methods have been proposed for site characterization and leak detection monitoring. Song *et al.*[15] studied the feasibility of monitoring using a surface wave seismic method and concluded that it is very difficult to detect abnormalities using this method alone. In recent years, the microseismic monitoring technique has been proposed and tested for demonstrating the safety of CO_2 storage at sequestration sites in a cost-effective manner.[16,17] Bohnhoff *et al.* utilized a passive seismic monitoring network consisting of two arrays of three-component sensors in two monitoring wells to detect CO_2 leakage along monitoring wellbores at a pilot carbon sequestration experiment in the Michigan Basin.[18,19] Unusual microseismic events were found and believed to be associated with the degassing processes of CO_2 when migrating upward along the monitoring wells. The microseismic monitoring technique has also been carried out at a CO_2-Enhanced Oil Recovery (EOR) pilot project and found useful for CO_2 and CH_4 leakage detection by applying seismological processing schemes to continuous seismic waveform recordings in a two-week period.[20] Our study focuses on the performance and detection power of a particular deep-subsurface seismic method, controlled-source seismic measurements above the reservoir caprock.

Seismic monitoring has been commonly applied in oil and gas reservoir characterization and for monitoring changes in reservoir rock properties remotely.[21] It has also been implemented in several pilot CO_2 sequestration sites, such as the Frio Formation near Houston and the Penn West CO_2-EOR site.[22–24] Different seismic monitoring methods, including time-lapse 2D or 3D surface seismic surveys, borehole vertical seismic profiling and cross-well seismic monitoring, have been employed at sequestration sites.[22–25] The seismic attributes that can be measured include seismic velocity, travel time, amplitude and impedance.[23] In our study, predicted changes in seismic velocity and travel time after CO_2 leakage events occur are considered.

Extensive studies have been undertaken to model CO_2 leakage from sequestration sites. The governing equations controlling these processes are the mass and energy balance equations, which can be solved analytically under simplified assumptions or numerically by space and time discretization. Nordbotten *et al.*[26] developed analytical solutions for modeling CO_2 leakage through multiple abandoned wells. There have also been numerical simulators, such as TOUGH2 and STOMP, developed to model multiphase flow in the subsurface.[27,28] The application of the TOUGH2 simulator in modeling CO_2 leakage has been demonstrated in several studies.[6, 29–32]

At geological sequestration sites, CO_2 is injected into formations usually more than 1000 m deep. Under the conditions encountered in sequestration reservoirs, CO_2 is in the supercritical fluid phase. To model changes in seismic velocity and seismic travel time after fluid substitution, the Biot-Gassmann equation[33] is commonly used.[21,34] Gutierrez *et al.*[35] studied the effects of CO_2 injection on the seismic velocity of sandstone and confirmed that the Biot-Gassmann substitution theory can be used in modeling changes in the P-wave velocity of sandstone containing supercritical CO_2 and saline water when the distribution of the two fluids in the pore space is accounted for in the calculation.

Uncertainty quantification in modeling CO_2 leakage is crucial in regulatory compliance assessment.[36] The uncertainty can be attributed to natural variability within the physical system, incomplete knowledge of model input parameters caused by insufficient or inaccurate site characterization, and simplifications of the physical model.[36] Leakage detectability has been assessed through the signal-to-noise ratio using the probabilistic collocation method.[37] Oladyshkin *et al.*[38] developed a methodology for data-driven uncertainty quantification using polynomial chaos expansion (PCE) and applied it to modeling CO_2 storage in geological reservoirs. The PCE approach, an efficient and flexible uncertainty quantification technique, allows uncertainty analysis of complex and computationally intensive models to be conducted with relatively low computation time.[12,39] A response surface approach using the multivariate adaptive regression spline (MARS)[40,41] was employed to estimate wellbore leakage rates of CO_2 and brine from storage reservoirs.[42] For CO_2 leakage through a fault,

the uncertainties in estimated leakage rates or aquifer chemistry were assessed using polynomial functions as reduced-order models.[43,44] Reduced order models have also been used to evaluate the impacts of CO_2 leakage on shallow groundwater resources by several authors.[45,46] Generally applicable problem-solving environments for uncertainty analysis and design exploration (PSUADE),[41] have been developed and integrated into a system-level risk analysis tool.[42–44] In our study, the uncertainty of the calculated seismic travel time is analyzed using the arbitrary PCE method[47] combined with Monte Carlo simulation. The PCE model serves as a stochastic response surface for the numerical simulation results from TOUGH2.

The objective of this study is to evaluate the detection power of seismic travel time measurements at different CO_2 leakage rate levels. A simplified rock physics model is assumed for monitoring zones at sequestration sites. Changes in pore pressure and CO_2 saturation at different leakage levels are estimated using the TOUGH2 numerical simulator. The model results are then approximated by the PCE method. Monte Carlo uncertainty analysis is performed for seismic travel time using the Biot-Gassmann equation and the estimated pressure and CO_2 saturation from the fitted PCE models. A methodology for conducting a statistical power analysis is developed and demonstrated based on the ability to distinguish between P-wave travel times with and without pressure and CO_2 saturation changes modeled as a result from CO_2 leakage. The empirical distributions of detection power are obtained at four leakage levels from the Monte Carlo uncertainty analysis.

Modeling changes in seismic travel time

Model set-up

The monitoring zone where the seismic source and receiver are located is modeled as a homogenous layer at a depth of 1 km below the ground surface. The CO_2 would be in the supercritical phase partially saturating the pore space throughout the monitoring zone under the temperature and pressure conditions at this depth. The geometry of the simplified rock physics model for the monitoring zone is illustrated in Figure 1. The lithology type is sandstone with a density of 2600 kg/m^3. The lateral extent of the model domain is 10 km and the thickness of the monitoring zone is 50 m. The model domain is discretized with a mesh of $80 \times 5(400)$ grids. The mesh is refined around the leakage point with a grid width of 50 m. The grid width 1 km farther away from the leakage point is 200 m. The CO_2 leakage point is at the center bottom of the monitoring zone. The temperature is constant at 45 °C and the gradient of initial hydrostatic pressure is 0.1 bar/m. Two-phase (supercritical CO_2 and brine) flow has been considered in the model. van Genuchten functions[48] are adopted to estimate the capillary pressure. The parameters of van Genuchten functions are listed in the Supporting Information.

The initial CO_2 saturation in the pore space is assumed to be zero. The monitoring zone is initially filled with brine with a salinity of 0.15 in weight fraction. The point source of the seismic signal is located at the top of the monitoring zone and the receiver is directly below the source at the bottom of

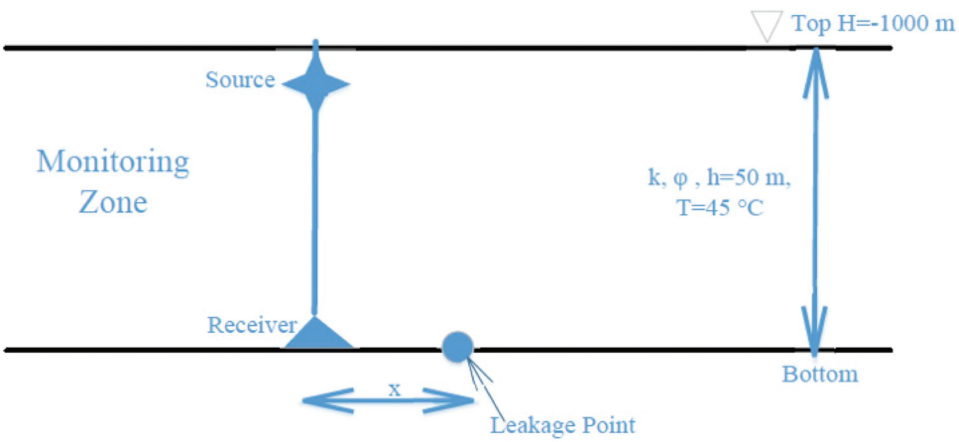

Figure 1. Geometry of the simplified rock physics model for the monitoring zone.

Table 1. Symbols and values for parameters of the modeled monitoring zone.

Parameter	Symbol	Value
Depth below the ground surface (m)	H	1000
Thickness (m)	h	50
Temperature (°C)	T	45
Initial pressure (MPa)	P_initial	Uncertain
Permeability (mD)	k	Uncertain
Porosity (%)	φ	Uncertain
Initial CO_2 saturation	Sg_initial	0
Density of rock (kg/m^3)	ρ	2600
Salinity of brine (weight fraction)	S	0.15
CO_2 leakage rate (tonnes/year)	LR	10, 50, 100, and 150
Distance of monitor from leakage point (m)	x	0 or 500

the monitoring zone. The source and the receiver thus form a vertical line perpendicular to the bottom. The signal recorded is the direct arrival from the top to the bottom of the monitoring zone. The horizontal distance between the receiver and the leakage point is x, which is assumed to be either 0 or 500 m, respectively in this study. The permeability, porosity and initial pressure at the top of the monitoring zone are uncertain input parameters with empirical distributions defined in the section Stochastic response surface method. The symbols and values for parameters of the modeled monitoring zone are summarized in Table 1. Note that the CO_2 storage reservoir and the leakage pathway are not explicitly modeled in this study. It is assumed that 10^5 tonnes of CO_2 has been injected into the storage reservoir and the migrating CO_2 has reached the center bottom of the monitoring zone through a high permeability conduit in the caprock.

Calculation of seismic velocity and travel time

Based on the laboratory study of rock samples conducted by Wang *et al.*,[49] changes in seismic velocity are mainly due to changes in pressure and CO_2 saturation in the pore space. The pressure and CO_2 saturation for the no-leakage case and the four leakage rate levels (i.e., small, moderate, large and very large) are estimated using the TOUGH2/ECO2N module.[50] The CO_2 leakage rates that correspond to the four leakage levels are 10 tonnes/year, 50 tonnes/tear, 100 tonnes/year, and 150 tonnes/year. The small leakage level (i.e., 10 tonnes/year) represents a scenario where 1% of injected CO_2 is leaking from a storage reservoir containing 10^5 tonnes of CO_2 over 100 years.

Seismic wave velocity in the monitoring zone is estimated using the moduli and density of the rock:

$$V_p = \sqrt{\frac{K_{sat} + \frac{4}{3}\mu}{\rho_{sat}}} \tag{1}$$

$$V_s = \sqrt{\frac{\mu}{\rho_{sat}}} \tag{2}$$

where V_p and V_s are the P- and S-wave velocity; K_{sat} and μ are the bulk and shear moduli of the rock; and ρ_{sat} is the density of the rock.

The bulk modulus of a saturated rock is computed using the Gassmann equation:[33]

$$K_{sat} = K_{frame} + \frac{\left(1 - \frac{K_{frame}}{K_{matrix}}\right)^2}{\frac{\varphi}{K_{fl}} + \frac{1-\varphi}{K_{matrix}} - \frac{K_{frame}}{K_{matrix}^2}} \tag{3}$$

where K_{sat}, K_{frame}, K_{matrix}, and K_{fl} are the bulk moduli of the saturated rock, porous rock frame, mineral matrix and pore fluid, respectively. φ is the porosity of the rock as a fraction. The shear modulus is held constant during the fluid substitution in the Gassmann theory. The bulk and shear moduli of the rock frame are estimated using the Hertz-Mindlin contact theory for consolidated rock and the Hashin-Shtrikman bounds.[51,52] The equations are included in the Supporting Information. The density of the rock is calculated with the volume averaging equation:

$$\rho_{sat} = \varphi\rho_{fl} + (1-\varphi)\rho_{matrix} \tag{4}$$

where ρ_{fl} and ρ_{matrix} are the density of the fluid phase and the density of the mineral matrix, respectively.

For a formulation and Matlab codes that implement the Gassmann fluid substitution theory, the readers are referred to Kumar.[34]

Once the gridded fields of seismic velocities are determined, the direct travel time along the vertical wave path from top to bottom is computed as:

$$t = \int_0^h \frac{1}{v} dz \tag{5}$$

where v is the seismic velocity and h is the thickness of the monitoring zone.

Uncertainty quantification and power analysis

The uncertainty of the seismic travel time is estimated using the Monte Carlo method. As the computation time of the TOUGH2 simulation is too large to directly implement the Monte Carlo method with a sufficient sample size, a stochastic response surface using the polynomial chaos expansion is fitted to the TOUGH2 outputs (i.e., pressure and CO_2 saturation), allowing more rapid Monte Carlo evaluation of this surrogate model.

Stochastic response surface method

The stochastic inputs in the uncertainty analysis are permeability, porosity and initial pressure at the top of the monitoring zone. The empirical distributions of permeability and porosity are obtained from the US National Petroleum Council (NPC) database, which contains the raw data for over one thousand reservoirs.[53] The initial pressure is sampled independently of the permeability and porosity pairs. While porosity and pressure are expected to exhibit some degree of negative correlation (since formations at greater depth should exhibit somewhat lower porosity and higher pressure), a correlation coefficient of only −0.13 was determined from the NPC database, small enough to yield only a small effect on the subsequent simulation results (especially since it is the change in pressure, rather than the pressure itself that affects observable changes in seismic velocity). A very small correlation coefficient (−0.04) was also determined between permeability and initial pressure. Scatter plots of permeability vs. initial pressure data and porosity vs. initial pressure data in the NPC database are provided in the Supporting Information.

Although the NPC database also contains initial pressure data for reservoirs, they are at various depth and lithology types. In our model setting, the top of the monitoring zone is fixed at a depth of 1 km and the lithology type of the monitoring zone is sandstone. Therefore, a synthetic dataset for initial pressure at a depth of 1 km and sandstone reservoirs is generated based on the initial pressure data in the NPC database. The distribution of initial pressure is assumed to be a truncated normal with a mean of 9.68 MPa and a standard deviation of 3.94 MPa before the truncation. The lower and upper limits of the truncated normal distribution are 1.93 MPa and 17.42 MPa, respectively. The procedure for generating the synthetic dataset for initial pressure from the truncated normal distribution is shown in the Supporting Information. Figure 2 illustrates the empirical distributions of the three uncertain input parameters. With this approach the empirical distributions of permeability, porosity and initial pressure across all (or, as described below, selected subsets) of the reservoirs in the NPC database are used to prescribe the variation across the parameter space for individual (randomly selected) sites.

The pressure and CO_2 saturation outputs from the TOUGH2 simulation at each leakage level are approximated by PCE on the set of uncertain input parameters $\{\omega_i\}_{i=1}^n$ given by:

$$y = a_0 + \sum_{i1=1}^{n} a_{i1}\Gamma_1(\omega_{i1}) + \sum_{i1=1}^{n}\sum_{i2=1}^{i1} a_{i1i2}\Gamma_2(\omega_{i1},\omega_{i2}) + \sum_{i1=1}^{n}\sum_{i2=1}^{i1}\sum_{i3=1}^{i2} a_{i1i2i3}\Gamma_3(\omega_{i1},\omega_{i2},\omega_{i3}) + \ldots \tag{6}$$

where y is an output (either pressure or CO_2 saturation) of the TOUGH2 model; $a_{i1\ldots}$ are coefficients to be estimated; and the $\Gamma_p(\omega_{i1},\ldots,\omega_{ip})$ are multidimensional polynomial basis functions that are orthogonal in the input space.

The multidimensional polynomial basis functions $\Gamma_p(\omega_{i1},\ldots,\omega_{ip})$ are constructed using the arbitrary polynomial chaos expansion (aPC) approach of Oladyshkin and Nowak.[47] The set of aPC basis functions is constructed from the moments of the uncertain input variables. The equations used to construct the aPC basis are provided in the Supporting Information. The aPC approach allows the use of empirical datasets to represent input uncertainties, which avoids errors introduced by fitting standard parametric statistical distributions to empirical datasets. The coefficients ($a_{i1\ldots}$) of the polynomial basis can be estimated by the probabilistic collocation method[54,55] or a statistical regression method.[36,39]

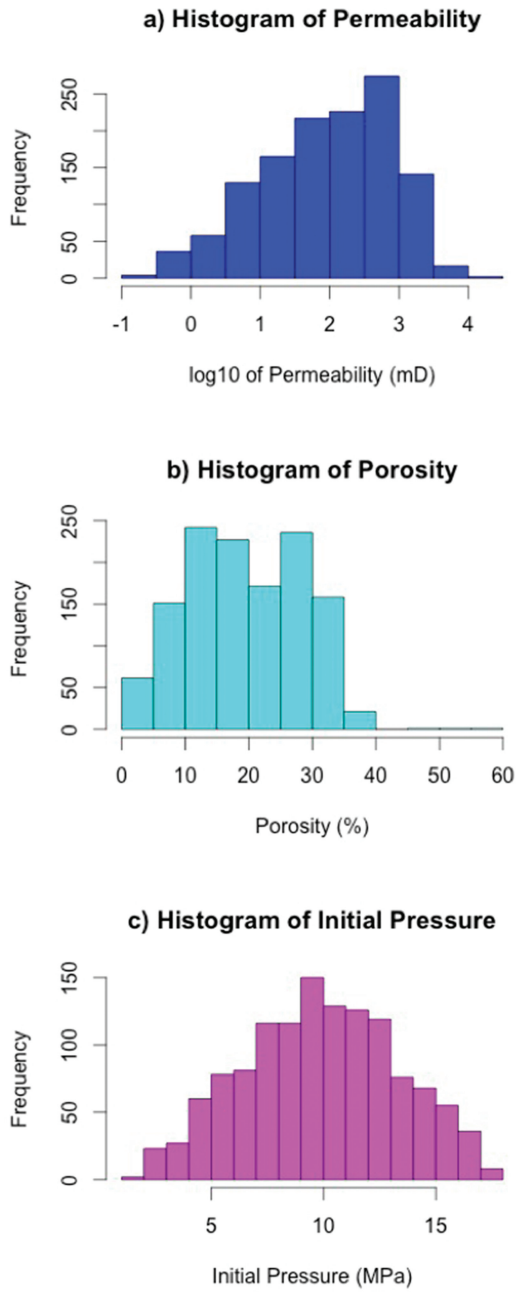

Figure 2. Histograms of stochastic inputs: (a) Permeability; (b) Porosity; and (c) Initial pressure.

In this study, a third-order polynomial expansion function is chosen to approximate the TOUGH2 outputs. As there are three uncertain input parameters (n = 3) and the order of the expansion is three (d = 3), the total number of terms (M) in the polynomial expansion function is 20, according to the combinatory formula:

$$M = \frac{(n+d)!}{n!d!} \tag{7}$$

The coefficients of the polynomial basis are estimated using the probabilistic collocation method,[54] which requires evaluating the TOUGH2 model with M different sets of uncertain input parameters $\{\omega_i\}_{i=1}^{n}$ that are called collocation points. The collocation points are selected from the high probability roots of the $(d+1)$th (i.e., fourth in this study) order orthogonal polynomial for each uncertain input parameter. At each leakage level, 20 runs of the TOUGH2 model are needed to solve the 20 coefficients in the polynomial expansion function. The PCE models are constructed at each element in the model domain for each output variable (i.e., pressure and CO_2 saturation), resulting in a total of $(80\times5)\times2=800$ polynomial functions at each specific time and leakage level.

Monte Carlo uncertainty analysis

Once the PCE models are constructed, the seismic velocity at each element in the model domain can be calculated at a relatively low computational cost, which facilitates Monte Carlo uncertainty analysis. For each set of uncertain input parameters introduced in the section Stochastic response surface method, combined with the fixed parameters in Table 1, the direct seismic travel time from the top to bottom of the formation at locations x = 0 m and 500 m are calculated for the no-leakage case and the four leakage levels, at t = 1, 5, 10 and 50 years, respectively. The empirical distributions of changes in seismic travel time (Dt) at four leakage levels are obtained by subtracting the travel time for the no-leakage case (T_0) from the travel time at each leakage level (T_i, i = 1,4).

$$Dt = T_i - T_0 \tag{8}$$

where i = 1 for small leak, 2 for moderate leak, 3 for large leak and 4 for very large leak

Power analysis

To assess the power of CO_2 leakage detection using seismic travel time, a statistical hypothesis test is assumed to be performed on measured changes in travel time (Dt_m) at each leakage level. The null and alternative hypotheses are given by:

$$H_0 : Dt_m \le 0 \left(no\,leak\right) \tag{9}$$

$$H_1 : Dt_m > 0 \left(a\,leakage\,event\,occurs\right)$$

As travel time changes of 0.2 to 1.0 ms can be observed using a continuous active-source seismic

monitoring technique,[22] the standard deviations of measurement errors of the seismic travel times (T_0 and T_i) are assumed to be 0.2 ms in the hypothesis test, corresponding to a coefficient of variation of 0.2 to 1 in the study by Daley *et al.*[22] The distribution of measured seismic travel time is thus assumed to be normal with a mean of the simulated value from the Monte Carlo uncertainty analysis and a standard deviation of 0.2 ms, which is the assumed standard deviation of measurement errors (σ_e). Therefore, the measured changes in seismic travel time (Dt_m) at each leakage level also follow the normal distribution:

$$T_{i,m} \sim N(T_{i,s}, \sigma_e)$$

$$T_{0,m} \sim N(T_{0,s}, \sigma_e)$$

$$Dt_m = (T_{i,m} - T_{0,m}) \sim N(\mu, \sigma) \quad (10)$$

where: $\mu = T_{i,s} - T_{0,s}$

$$\sigma = \sqrt{2} \times \sigma_e$$

The hypothesis test (Eqn (9)) tests whether the mean of the measured changes in travel time (Dt_m) is statistically significantly different from zero. If it is, the null hypothesis (i.e., the no-leakage case) is rejected and we conclude that the measured travel times provide sufficient evidence of a leakage event. The critical value of Dt_m for the hypothesis test is chosen to be $Dt_{cri} = 2\sigma$, corresponding to a significance level of about 0.02 for the test of hypothesis. The power of the hypothesis test for CO_2 leakage detection is computed as the probability that Dt_m is larger than Dt_{cri} when a leakage event occurs (at each of the four leakage levels). Note that a group of measurements of changes in seismic travel time is assumed to be made, after which the mean of the observed values will be compared to Dt_{cri}. However, since these measurements (and their errors with respect to leakage effects and inference) are expected to be highly correlated, the effective sample size is conservatively assumed to be one.

Results and discussion

Predicted seismic velocity in model domain

Seismic velocities, including the P-wave velocity and the S-wave velocity, at each element in the model domain are calculated using the predicted pressure and CO_2 saturation values from the PCE models, combined with the Biot-Gassmann model for fluid substitution introduced in the section Calculation of seismic velocity and travel time. Figure 3 shows the model results for the no-leakage case and the moderate leakage level at t = 10 year. In this figure, the values of the three uncertain input parameters are as follows: permeability = 100 mD, porosity = 15% and initial pressure = 9.5 MPa. The results at t = 1, 5, and 50 year and at different leakage levels are shown in the Supporting Information.

The velocity of the P-wave decreases by about 7.5% around the leakage point at the moderate leakage level after 10 years of leakage. The effect of the decreased P-wave velocity propagates upwards in the center towards the top of the monitoring zone. For the areas at the bottom of the monitoring zone but far away from the center, the P-wave velocity decreases by about 3.7%. Discontinuities in the P-wave velocity occur at distances beyond 1000 m from the point of leakage; however these do not influence the estimates that follow, as the estimates are made for monitors located at x = 0 or x = 500 m from the leakage point. In general, as the leakage level and time increases, the drop in the P-wave velocity gets larger and affects larger areas in the monitoring zone. The decrease in P-wave velocity is the competing effects of pore pressure and CO_2 saturation increase after CO_2 leakage occurs in the monitoring zone.

The S-wave velocity changes little, increasing slightly around the leakage point by about 0.8% at the moderate leakage level after 10 years of leakage. The maximum increase in S-wave velocity at all the leakage levels considered in this study is about 1% (at the very large leakage level). The effect of CO_2 saturation on the changes in S-wave velocity is caused mainly by the change in the density of the pore fluid. The shear modulus of the rock is not affected by CO_2 saturation because the shear modulus of fluids is zero. Pore pressure has an impact on both the shear modulus of the rock and the density of the pore fluid. As the changes in S-wave velocities are too small to serve as a basis for leakage detection, the S-wave travel time is excluded from further analysis.

Detection power using P-wave travel time

Monte Carlo uncertainty analysis is performed for the P-wave travel time along a vertical wave path from the top to the bottom of the formation (Figure 1) at

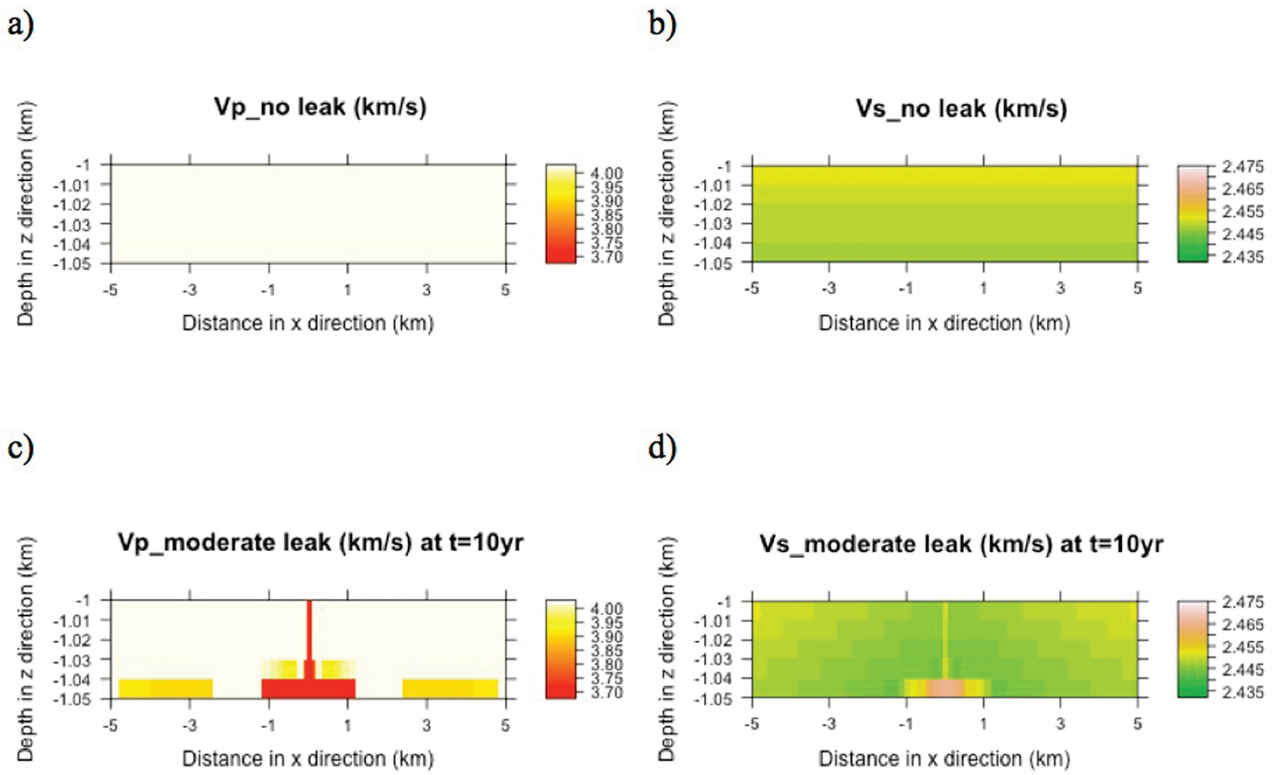

Figure 3. Sample model results of P-wave (a and c) and S-wave (b and d) seismic velocities for the no-leakage case (a and b) and the moderate leakage level (c and d) at t = 10 year ($k = 100\ mD$, $\varphi = 15\%$, $P\_initial = 9.5\ MPa$) .

locations x = 0 and 500 m respectively, from the point of leakage. The input parameter space is divided into four regions based on permeability and porosity ranges, as in practice, the permeability and porosity ranges of the monitoring zone could be known in advance by site characterization. Four primary groups are identified in the input permeability-porosity space from the NPC database, denoted by different colors in Figure 4. In addition, initial pore pressures are sampled independently for each case from the assumed truncated normal distribution shown in Figure 2(c). The group of points in red represents inputs with low porosity. The groups of points in green, orange and purple represent inputs with relatively high porosity, and with low, moderate and high permeability, respectively. Figures 5–7 show the resulting computed empirical cumulative distribution function (CDF) of detection power using the P-wave travel time at the location x = 0 m (center of the monitoring zone) for the four regions in the input permeability-porosity space at t = 5, 10 and 50 year, respectively. The results for the location x = 500 m and those at t = 1 year are shown in the Supporting Information.

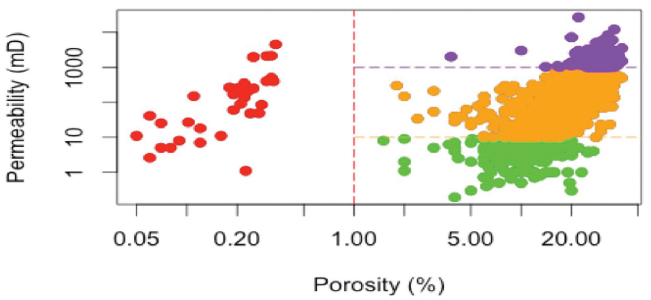

Figure 4. Scatter plot of permeability vs. porosity input parameters used in the Monte Carlo simulation. Each point represents an observation in the US National Petroleum Council (NPC) database. The observations are classified into four regions of the parameter space as indicated by color.

It is evident that the detection power of the test of hypothesis for decreases in the P-wave travel time differs for different regions of the permeability – porosity input space. The P-wave travel time test exhibits good power for CO_2 leakage detection if the permeability and porosity of the monitoring zone are

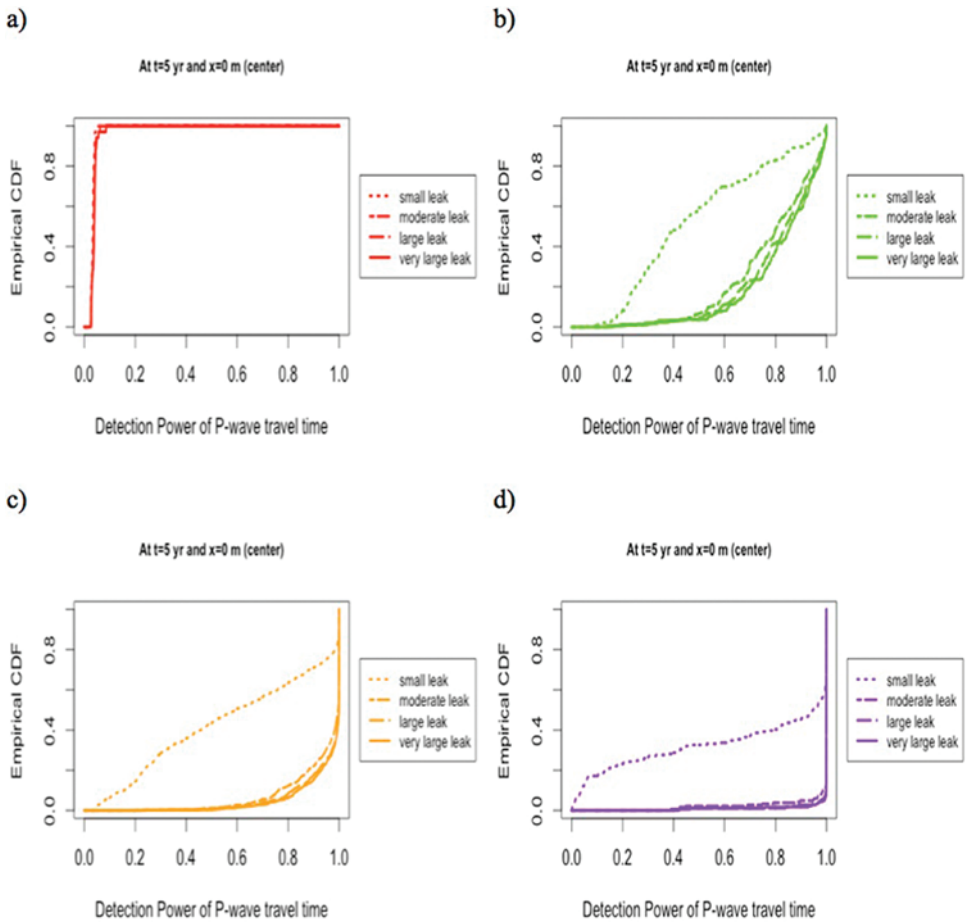

Figure 5. Empirical CDF of detection power of P-wave travel time test of hypothesis (Eqn (9), at significance level $\alpha = 0.02$) at four leakage levels, t = 5 year, x = 0 m and at (a) low porosity region (red points in Fig. 4); (b) high porosity and low permeability region (green points in Fig. 4); (c) high porosity and moderate permeability region (orange points in Fig. 4); and (d) high porosity and high permeability region (purple points in Fig. 4).

relatively high (purple curves in Figures 5–7(d)). The detection power using the P-wave travel time test is very low for monitoring zones with low porosity, no matter the value of the permeability value (red curves in Figures 5–7(a)). For monitoring zones with porosity larger than 1% (green, orange, and purple regions in Figure 4), the detection power using the P-wave travel time test is generally higher for a high permeability formation than for a low permeability layer. The detection power increases with increasing time since the leakage occurs. For example, comparing Figure 5(c) to Figure 7(c), the probability of achieving a detection power larger than 0.8 at the small leakage level increases from 0.4 (at t = 5 year) to about 0.82 (at t = 50 year) if the permeability and porosity ranges of the monitoring zone fall into the orange region in Figure 4. As shown in Figure 7(d), high detection power using the P-wave travel time test can be achieved for monitoring zones with high permeability at t = 50 year. Comparing the results at x = 0 m to those at x = 500 m, it is seen that the detection power is higher at the location closer to the leakage point (x = 0 m) than at the location farther away (x = 500 m). The detection power does not change much for different CO_2 leakage levels at the location x = 0 m. However, at the location x = 500 m, a higher leakage level is necessary before a detection based on the seismic wave velocity is likely to occur.

The expected detection power using the P-wave travel time test of hypothesis for different regions of

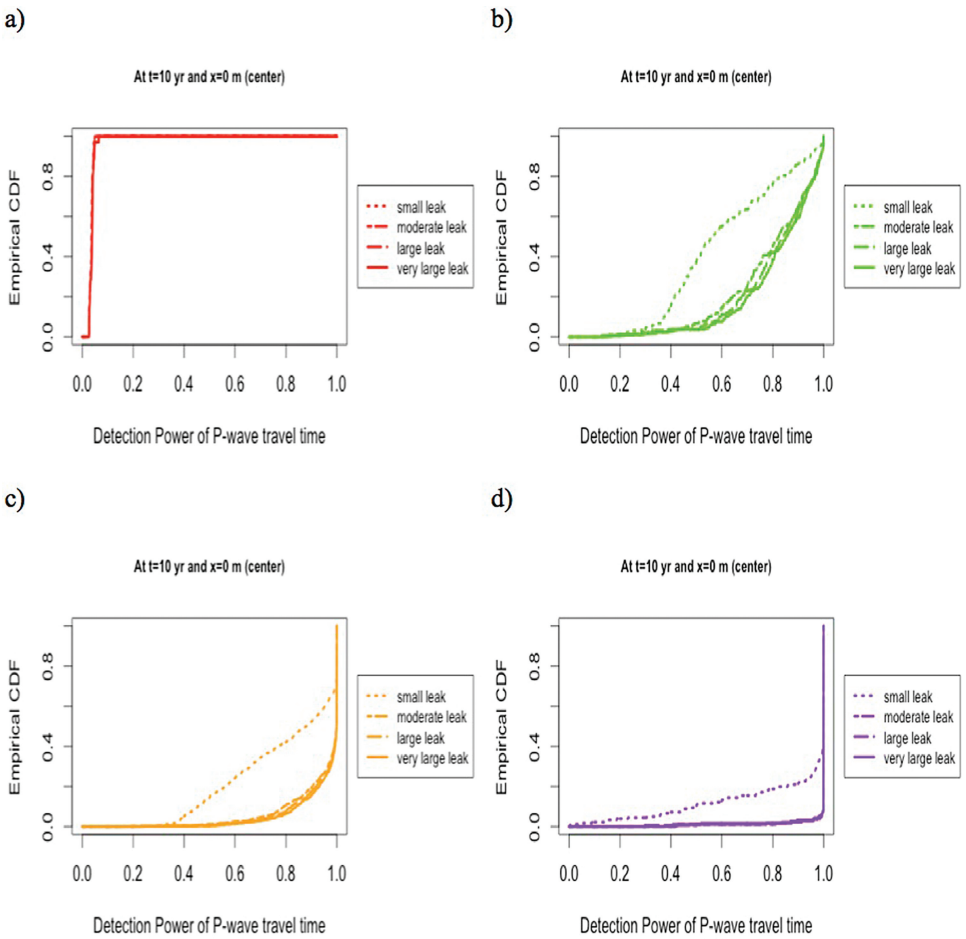

Figure 6. Empirical CDF of detection power of P-wave travel time test of hypothesis (Eqn (9), at significance level $\alpha = 0.02$) at four leakage levels, t = 10 year, x = 0 m and at (a) low porosity region (red points in Fig. 4); (b) high porosity and low permeability region (green points in Fig. 4); (c) high porosity and moderate permeability region (orange points in Fig. 4); and (d) high porosity and high permeability region (purple points in Fig. 4).

the permeability and porosity input space at the location x = 0 m and at four leakage levels is illustrated in Figure 8 as a function of time since the leakage occurs. Under the assumed uncertainty in the input parameters and the specified geometry of the rock physics model, the detection power remains low, especially for a small or moderate leak, until after five years of leakage has occurred. For monitoring zones with low porosity (red lines in Figure 8), the expected power for detecting small leakage events is very low regardless of time. For small leakage rates at high porosity sites, higher permeability does lead to increased power, though at higher leakage rates these differences are no longer apparent, since high power is achieved in all cases with high porosity (irrespective of permeability) after five or more years of leakage.

Discussion

The conceptual model used in our analysis for the subsurface seismic monitoring zone is highly simplified, assuming homogeneous porosity and permeability, a single fixed leakage source, and known spatial dimensions; with variation across sites captured in the distribution of reported average (or, representative) porosity and permeability. This approach was taken to provide a relatively simple and tractable basis upon which a framework for power analysis could be built and demonstrated, involving: (i) simulation of

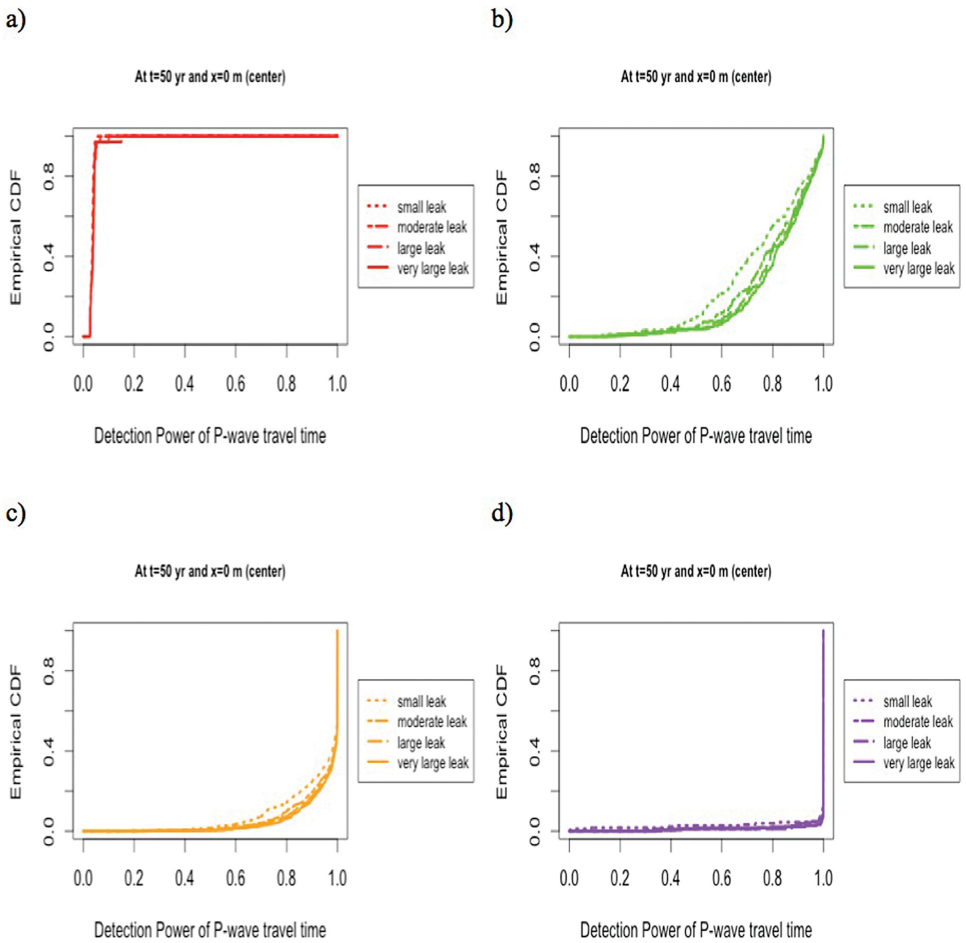

Figure 7. Empirical CDF of detection power of P-wave travel time test of hypothesis (Eqn (9), at significance level $\alpha = 0.02$) at four leakage levels, t = 50 year, x = 0 m and at (a) low porosity region (red points in Fig. 4); (b) high porosity and low permeability region (green points in Fig. 4); (c) high porosity and moderate permeability region (orange points in Fig. 4); and (d) high porosity and high permeability region (purple points in Fig. 4).

the pressure and CO_2 saturation response to leakage in the monitoring zone; (ii) calculation of the resulting effect on seismic wave velocities; (iii) consideration of the effect of monitoring measurement error; and (iv) evaluation of the resulting statistical distribution of monitored seismic wave velocities under the null (no leakage) and alternative (leakage of different magnitudes) hypotheses. While we believe that the results for different types of reservoirs (colors in Figures 4–8) provide useful initial insights into which are likely to have the potential for effective seismic wave monitoring for leak detection, it is the development of this overall conceptual framework that is the major contribution of the paper. When applied at actual sites, the framework will require consideration of reservoir heterogeneity, with spatially varying (and uncertain) distributions of porosity, permeability and other features at the site. Methods to simulate uncertain subsurface spatial fields conditioned on partial observations of permeability and other measurements are available using approaches that rely on knowledge of subsurface processes and statistical techniques such as Sequential Gaussian Simulation.[56–58] We look forward to using methods such as these to evaluate seismic monitoring and other leak detection methods at a test site at some time in the future.

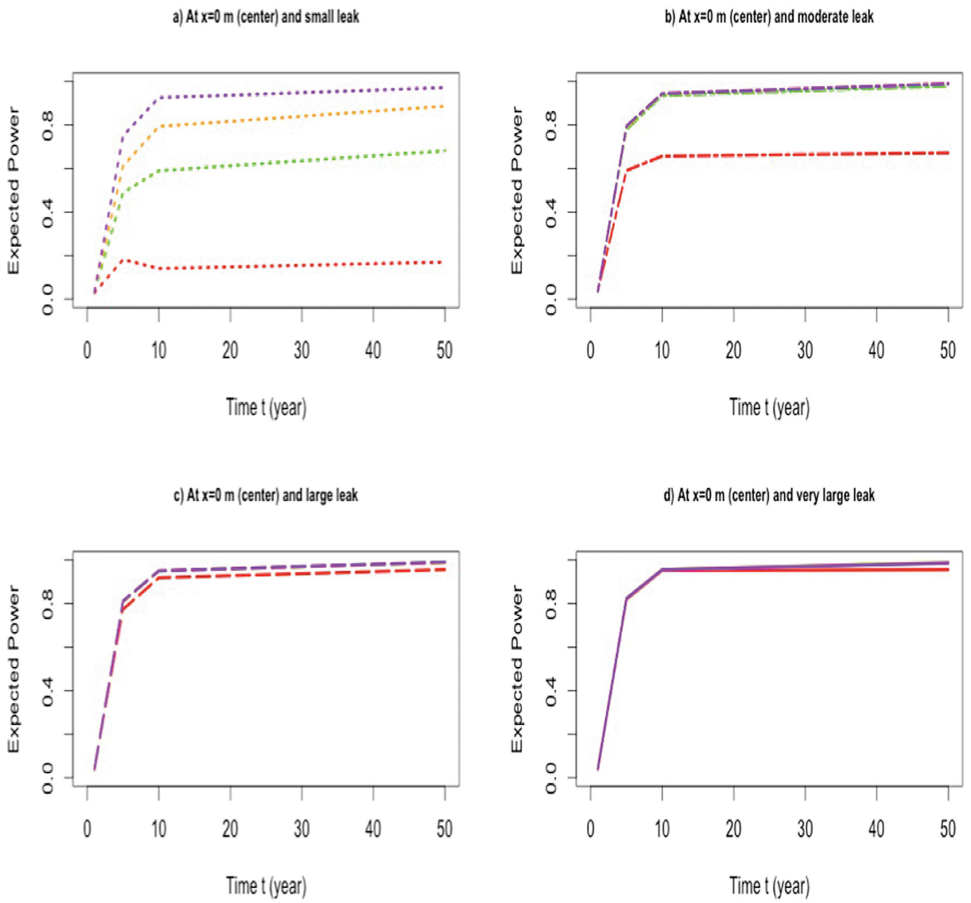

Figure 8. Expected detection power of P-wave travel time test of hypothesis (Eqn (9), at significance level $\alpha = 0.02$) as a function of time since leakage for four regions of the permeability and porosity input space (the red, green, orange and purple regions in Fig. 4, denoted by colored lines in Fig. 8), at the location x = 0 m and at (a) small leakage level; (b) moderate leakage level; (c) large leakage level; and (d) very large leakage level.

Conclusions

In this work, the power of CO_2 leakage detection using a statistical analysis and test of P-wave travel times is assessed with a simplified rock physics model for the monitoring zone. The empirical distributions of detection power using the P-wave travel time for four regions in the permeability-porosity input space at four leakage levels are obtained from the Monte Carlo uncertainty analysis with a stochastic response surface method. For a reservoir with intermediate values of porosity, permeability and initial pressure, the model results predict that the P-wave velocity decreases by about 7.5% around the leakage point 10 years after the initiation of a moderate leakage rate. The detection power using the P-wave travel time measurements and test alone is generally not high enough for small leakage events, unless the porosity and the permeability of the monitoring zone are high, and/or a long period of time has elapsed since the leakage occurred. The results indicate that there is an advantage to choosing a monitoring zone with high porosity and high permeability for the purpose of monitoring CO_2 leakage with seismic wave velocity detection. The detection power is higher when the leak occurs near the location of the monitoring system, suggesting the possible need for multiple monitoring locations when the reservoir and the monitoring zone are large. As the likely pathways for concentrated CO_2 leakage at sequestration sites include abandoned wells and faults, the seismic monitoring equipment may be most effectively

deployed along the abandoned wells or above the faults (if any are present). As the sole measurement of the P-wave travel time cannot provide sufficient power for CO_2 leakage detection in many cases, measurements from other monitoring techniques, such as pressure monitoring and near-surface monitoring will likely need to be combined at sequestration sites to increase the probability that leakage events are detected and addressed in a timely manner.

Acknowledgements

As part of the National Energy Technology Laboratory's Regional University Alliance (NETL-RUA), a collaborative initiative of the NETL, this technical effort was performed under the RES contract DE-FE0004000. We would like to thank Professor William Harbert at University of Pittsburgh for providing thorough and constructive reviews. We would also like to thank the reviewers for their valuable suggestions.

References

1. Ciais P, Sabine C, Bala G, Bopp L, Brovkin V, Canadell J *et al*., Carbon and Other Biogeochemical Cycles. In: Climate Change 2013: The Physical Science Basis. Contribution of Working Group I to the Fifth Assessment Report of the Intergovernmental Panel on Climate Change [Stocker, T.F., D. Qin, G.-K. Plattner, M. Tignor, S.K. Allen, J. Boschung, A. Nauels, Y. Xia, V. Bex and P.M. Midgley (eds.)]. Cambridge University Press, Cambridge, United Kingdom and New York, NY, USA (2013).
2. US DOE, *Carbon Sequestration Atlas of the United States and Canada*, 3rd ed. US DOE, National Energy Technology Laboratory, Morgantown, WV, USA (2010).
3. US DOE, *Monitoring, Verification, and Accounting of CO_2 Stored in Deep Geologic Formations*. US DOE, National Energy Technology Laboratory, Morgantown, WV, USA (2009).
4. Benson SM and Myer L, Monitoring to ensure safe and effective geologic storage of carbon dioxide. In: *Proceedings of the Intergovernmental Panel on Climate Change (IPCC) Wokshop on Carbon Dioxide Capture and Storage*. November 18-21, 2002, Regina, Saskatchewan, Canada (2002).
5. Yang Y-M, Small MJ, Ogretim EO, Gray DD, Bromhal GS, Strazisar BR *et al.*, Probabilistic design of a near-surface CO_2 leak detection system. *Environ Sci Technol* **45**(15):6380–6387 (2011).
6. Yang Y-M, Small MJ, Junker B, Bromhal GS, Strazisar B and Wells A, Bayesian hierarchical models for soil CO_2 flux and leak detection at geologic sequestration sites. *Environ Earth Sci* **64**(3):787–798 (2011).
7. Yang Y-M, Small MJ, Ogretim EO, Gray DD, Wells AW, Bromhal GS *et al.*, A Bayesian Belief Network (BBN) for combining evidence from multiple CO_2 leak detection technologies. *Greenh Gases Sci Technol* **2**(3):185–199 (2012).
8. Wang Z and Small MJ, A Bayesian approach to CO_2 leakage detection at saline sequestration sites using pressure measurements. *Int J Greenh Gas Control* **30**:188–196 (2014).
9. Azzolina NA, Small MJ, Nakles DV and Bromhal GS, Effectiveness of subsurface pressure monitoring for brine leakage detection in an uncertain CO_2 sequestration system. *Stoch Environ Res Risk Assess* **28**:895–909 (2014).
10. Birkholzer J, Zhou Q and Tsang C, Large-scale impact of CO_2 storage in deep saline aquifers: A sensitivity study on pressure response in stratified systems. *Int J Greenh Gas Control* **3**(2):181–194 (2009).
11. Chabora ER and Benson SM, Brine displacement and leakage detection using pressure measurements in aquifers overlying CO_2 storage reservoirs. *Energy Procedia* **1**(1): 2405–2412 (2009).
12. Sun AY, Zeidouni M, Nicot J-P, Lu Z and Zhang D, Assessing leakage detectability at geologic CO_2 sequestration sites using the probabilistic collocation method. *Adv Water Resour* **56**:49–60 (2013).
13. Sun AY, Nicot J-P and Zhang X, Optimal design of pressure-based, leakage detection monitoring networks for geologic carbon sequestration repositories. *Int J Greenh Gas Control* **19**:251–261 (2013).
14. Jung Y, Zhou Q and Birkholzer JT, Early detection of brine and CO_2 leakage through abandoned wells using pressure and surface-deformation monitoring data: Concept and demonstration. *Adv Water Resour* **62**:555–569 (2015).
15. Song X, Dai K, Chen G, Pan Y and Zhong Z, Sensitivity study of surface waves for CO_2 storage monitoring. *Int J Greenh Gas Control* **20**:180–188 (2014).
16. Verdon JP, Kendall J-M, White DJ, Angus D, Fisher QJ and Urbancic T, Passive seismic monitoring of carbon dioxide storage at Weyburn. *The Leading Edge* **29**(2):200–206 (2010).
17. Stork AL, Verdon JP and Kendall J-M, The microseismic response at the In Salah Carbon Capture and Storage (CCS) site. *Int J Greenh Gas Control* **32**:159–171 (2015).
18. Bohnhoff M and Zoback MD, Oscillation of fluid-filled cracks triggered by degassing of CO_2 due to leakage along well-bores. *J Geophys Res Solid Earth* **115**(11):1–29 (2010).
19. Bohnhoff M, Zoback MD, Chiaramonte L, Gerst JL and Gupta N, Seismic detection of CO_2 leakage along monitoring wellbores. *Int J Greenh Gas Control* **4**(4):687–697 (2010).
20. Martínez-Garzón P, Bohnhoff M, Kwiatek G, Zambrano-Narváez G and Chalaturnyk R, Microseismic monitoring of CO_2 injection at the Penn West Enhanced Oil Recovery pilot project, Canada: implications for detection of wellbore leakage. *Sensors* **13**(9):11522–11538 (2013).
21. Khatiwada M, Adam L, Morrison M and van Wijk K, A feasibility study of time-lapse seismic monitoring of CO_2 sequestration in a layered basalt reservoir. *J Appl Geophys* **82**:145–152 (2012).
22. Daley TM, Solbau RD, Ajo-Franklin JB and Benson SM, Continuous active-source seismic monitoring of injection in a brine aquifer. *Geophysics* **72**(5):A57–A61 (2007).
23. Alshuhail A and Lawton DC, Time-lapse surface seismic monitoring of injected CO_2 at the Penn West CO_2-EOR site, Violet Grove, Alberta. *CREWES Res Rep* **9**: 1–19 (2007).
24. Silver PG, Daley TM, Niu F, Majer EL. Active source monitoring of cross-well seismic travel time for stress-induced changes. *Bull Seismol Soc Am* **97**(1B):281–293 (2007).

25. Couëslan ML, Leetaru HE, Brice T, Scott Leaney W and McBride JH, Designing a seismic program for an industrial CCS site: Trials and tribulations. *Energy Procedia* **1**(1):2193–2200 (2009).
26. Nordbotten JM, Kavetski D and Celia MA, Model for CO_2 leakage including multiple geological layers and multiple leaky wells. *Environ Sci Technol* **43**(3):743–749 (2009).
27. Pruess K, Oldenburg C and Moridis G, TOUGH2 User's Guide, Version 2. University of California, Berkeley, CA (2012).
28. White MD, Watson DJ, Bacon DH, White SK, McGrail BP and Zhang ZF, STOMP: Subsurface Transport Over Multiple Phases. STOMP-CO2 and -CO2e Guide. US DOE, Pacific Northwest National Laboratory, Richland, Washington (2013).
29. Humez P, Audigane P, Lions J, Chiaberge C and Bellenfant G, Modeling of CO_2 leakage up through an abandoned well from deep saline aquifer to shallow fresh groundwaters. *Transp Porous Media* **90**(1):153–181 (2011).
30. Zheng L, Spycher N, Birkholzer J, Xu T, Apps J and Kharaka Y, On modeling the potential impacts of CO_2 sequestration on shallow groundwater: Transport of organics and co-injected H_2S by supercritical CO_2 to shallow aquifers. *Int J Greenh Gas Control* **14**:113–127 (2013).
31. Pruess K, On CO_2 fluid flow and heat transfer behavior in the subsurface, following leakage from a geologic storage reservoir. *Environ Geol* **54**(8):1677–1686 (2008).
32. Oldenburg CM and Unger AJA, On leakage and seepage from geologic carbon sequestration sites: unsaturated zone attenuation. *Vadose Zone J* **2**(3): 287–296 (2003).
33. Gassmann F, Über die elastizität poröser medien. *Vierteljahrsschrift der Naturforschenden Gesellschaft in Zürich* **96**:1–23 (1951).
34. Kumar D, A Tutorial on Gassmann Fluid Substitution: Formulation, Algorithm and Matlab Code. GEOHORIZONS January, 2006 (2006).
35. Gutierrez M, Katsuki D and Almrabat A, Use of the Biot-Gassmann equation in modeling of the seismic velocity changes during supercritical CO_2 injection in sandstone. *Poromechanics V*: Proceedings of the Fifth Biot Conference on Poromechanics. July 10-12, 2013, Vienna, Austria (2013).
36. Isukapalli SS and Roy A, Georgopoulosl PG. Stochastic response surface methods (SRSMs) for uncertainty propagation: Application to environmental and biological systems. *Risk Anal* **18**(3):351–363 (1998).
37. Sun AY, Zeidouni M, Nicot JP, Lu Z and Zhang D, Assessing leakage detectability at geologic CO_2 sequestration sites using the probabilistic collocation method. *Adv Water Resour* **56**:49–60 (2013).
38. Oladyshkin S, Class H, Helmig R and Nowak W, A concept for data-driven uncertainty quantification and its application to carbon dioxide storage in geological formations. *Adv Water Resour* **34**(11):1508–1518 (2011).
39. Zhang Y and Sahinidis NV, Uncertainty quantification in CO_2 sequestration using surrogate models from polynomial chaos expansion. *Ind Eng Chem Res* **52**:3121–3132 (2013).
40. Friedman JH, Multivariate adaptive regression splines. *Ann Stat* **19**(1):1–67 (1991).
41. Tong C, PSUADE Reference Manual (Version 1.3.0). Lawrence Livermore National Laboratory, Livermore, CA, May (2010).
42. Jordan AB, Stauffer PH, Harp D, Carey JW and Pawar RJ, A response surface model to predict CO_2 and brine leakage along cemented wellbores. *Int J Greenh Gas Control* **33**:27–39 (2015).
43. Sun Y, Tong C, Trainor-Guitton WJ, Lu C, Mansoor K and Carroll SA, Global sampling for integrating physics-specific subsystems and quantifying uncertainties of CO_2 geological sequestration. *Int J Greenh Gas Control* **12**:108–123 (2013).
44. Lu C, Sun Y, Buscheck TA, Hao Y, White JA and Chiaramonte L, Uncertainty quantification of CO_2 leakage through a fault with multiphase and nonisothermal effects. *Greenh Gases Sci Technol* **2**:445–459 (2012).
45. Dai Z, Keating E, Bacon D, Viswanathan H, Stauffer P, Jordan A *et al*., Probabilistic evaluation of shallow groundwater resources at a hypothetical carbon sequestration site. *Sci Rep* **4**(4006); DOI:10.1038/srep04006. (2014).
46. Zheng L, Carroll S, Bianchi M, Mansoor K, Sun Y and Birkholzer J, Reduced order models for prediction of groundwater quality impacts from CO_2 and brine leakage. *Energ Proc* **63**:4875–4883 (2014).
47. Oladyshkin S and Nowak W, Data-driven uncertainty quantification using the arbitrary polynomial chaos expansion. *Reliab Eng Syst Saf* **106**:179–190 (2012).
48. Van Genuchten MT, A closed-form equation for predicting the hydraulic conductivity of unsaturated soils. *Soil Sci Soc Am J* **44**: 892–898 (1980).
49. Wang Z, Cates ME and Langan RT, Seismc monitoring of a CO_2 flood in a carbonate resevoir: A rock physics study. *Geophysics* **63**(5): 1604–1617 (1998).
50. Pruess K, ECO2N: A TOUGH2 fluid property module for mixtures of water, NaCl, and CO_2. University of California, Berkeley, CA (2005).
51. Mavko G, Mukerji T and Dvorkin J, *The Rock Physics Handbook: Tools for Seismic Analysis in Porous Media*. Cambridge University Press, Cambridge, UK (2009).
52. Carcione JM, Picotti S, Gei D and Rossi G, Physics and seismic modeling for monitoring CO_2 storage. *Pure Appl Geophys* **163**(1): 175–207 (2006).
53. NPC (National Petroleum Council), US NPC Public Database (1984). Available at: http://www.netl.doe.gov/research/oil-and-gas/software/databases [May 5, 2014].
54. Tatang MA, Pan W, Prinn RG and McRae GJ, An efficient method for parametric uncertainty analysis of numerical geophysical models. *J Geophys Res* **102**:21925–21932 (1997).
55. Li H and Zhang D, Probabilistic collocation method for flow in porous media: Comparisons with other stochastic methods. *Water Resour Res* **43**(W09409):1–13 (2007).
56. Lengler U, De Lucia M and Kühn M, The impact of heterogeneity on the distribution of CO_2: numerical simulation of CO_2 storage at Ketzin. *Int J Greenh Gas Control* **4**(6):1016–1025 (2010).
57. Michael HA, Li H, Boucher A, Sun T, Caers J and Gorelick SM, Combining geologic process models and geostatistics for conditional simulation of 3-D subsurface heterogeneity. *Water Resour Res* **46**(W05527): 1–20 (2010).
58. Popova OH, Small MJ, McCoy ST, Thomas AC, Rose S, Karimi B *et al*., Spatial stochastic modeling of sedimentary formations to assess CO_2 storage potential. *Environ Sci Technol* **48**(11):6247–6255 (2014).

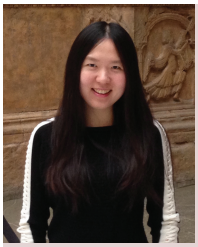

Zan Wang

Zan Wang is a PhD student at Department of Civil and Environmental Engineering at Carnegie Mellon University. Her main research focus is statistical analysis of CO_2 leakage detection at geological sequestration sites. Her research interests include statistical methods, uncertainty analysis, and environmental modeling.

Mitchell J. Small

Mitchell J. Small is the H. John Heinz III Professor of Environmental Engineering at Carnegie Mellon University. His research involves mathematical modeling of environmental systems, environmental statistics, risk assessment, and decision support.

